

hep-th/0501xxx  
FIT HE - 05-01  
KYUSHU-HET-80

# Flavor quark at high temperature from a holographic model

Kazuo Ghoroku<sup>†</sup>, Tomohiko Sakaguchi<sup>‡</sup> Nobuhiro Uekusa<sup>‡</sup> and  
Masanobu Yahiro<sup>‡</sup>

<sup>†</sup>Fukuoka Institute of Technology, Wajiro, Higashi-ku  
Fukuoka 811-0295, Japan

<sup>‡</sup>Department of Physics, Kyushu University, Hakozaki, Higashi-ku  
Fukuoka 812-8581, Japan

## Abstract

Gauge theory with light flavor quark is studied by embedding a D7 brane in a deconfinement phase background newly constructed. We find a phase transition by observing a jump of the vacuum expectation value of quark bilinear and also of the derivative of D7 energy at a critical temperature. For the model considered here, we also study quark-antiquark potential to see some possible quark-bound states and other physical quantities in the deconfinement phase.

---

<sup>†</sup>gouroku@dontaku.fit.ac.jp

<sup>‡</sup>tomohiko@higgs.phys.kyushu-u.ac.jp

<sup>‡</sup>uekusa@higgs.phys.kyushu-u.ac.jp

<sup>‡</sup>yahiro2scp@mbox.nc.kyushu-u.ac.jp

# 1 Introduction

It is still a challenging problem to make clear the gauge/gravity correspondence from superstring theory [1]. In particular, we expect that this correspondence is applicable to QCD by deforming the anti-de Sitter space-time (AdS) into an appropriate non-conformal form.

Recently an idea to add light flavor quarks has been proposed by Karch and Katz [2] for D3-D7 brane system in the  $\text{AdS}_5 \times S^5$  background. After that, several authors have extended this idea to various 10d gravity backgrounds corresponding to the various gauge duals, and they have examined the meson spectra and chiral symmetry breaking in the context of the holography [3, 4, 5, 6, 7, 8, 9, 10, 11]. There would be many directions to extend this idea. An interesting direction would be the analysis at finite temperature which is given in [4] for the D4-D6 model. However many things are left to be examined for the case of finite temperature.

Here we give such analyses in the background which is obtained as the extended solution to the finite temperature of the one given in [9]. The background given here corresponds to the Yang-Mills theory in the deconfining, high-temperature phase. The D7 brane is embedded in this background, and we could observe a gap of the vacuum expectation value of quark bilinear and also of the derivative of D7 energy with respect to the temperature. This implies a phase transition in the gauge theory at some temperature, and we discuss this point. And the problem related to the chiral symmetry is also discussed.

Through the estimation of the Wilson-Polyakov loop, we obtain a static quark-antiquark potential at finite-temperature, which is very similar to the one given by Rey, Theisen and Yee for the infinitely heavy quarks in the  $\text{AdS}_5 \times S^5$  background [12]. We also estimate the dynamical quark mass, and we discuss these results by comparing them with numerical results given in the recent lattice gauge simulations.

Especially, the potential obtained here implies that some meson states would remain until the temperature exceeds a critical value [13, 14], which is estimated here. A similar phenomenon is also seen for D5 baryon state at finite temperature. We discuss on these points.

In section 2, we give the setting of our model, and a phase transition is pointed out by embedding the D7 brane. In section 3, the quark-antiquark potential and the dynamical quark mass are studied through the Wilson-Polyakov loop estimations. In section 4, possible bound states for meson and baryon are discussed, and we also estimate the screening mass. The summary is given in the final section.

# 2 Background geometry

We solve the equations of motion for 10d IIB model under the Freund-Rubin ansatz for selfdual five form field strength,  $F_{\mu_1 \dots \mu_5} = -\sqrt{\Lambda}/2 \epsilon_{\mu_1 \dots \mu_5}$  [15, 16], and the following solution is obtained. The solution is written in the string frame and taking  $g_s = 1$ , as

follows,

$$ds_{10}^2 = G_{MN}dX^M dX^N = e^{\Phi/2} \left\{ \frac{r^2}{R^2} \left( -f^2(r)dt^2 + (dx^i)^2 \right) + \frac{1}{f^2(r)} \frac{R^2}{r^2} dr^2 + R^2 d\Omega_5^2 \right\}, \quad (1)$$

$$e^\Phi = \left( 1 + \frac{q}{r_T^4} \log\left(\frac{1}{1 - (r_T/r)^4}\right) \right), \quad \chi = -e^{-\Phi} + \chi_0, \quad (2)$$

$$f(r) = \sqrt{1 - \left(\frac{r_T}{r}\right)^4}, \quad (3)$$

where  $M, N = 0 \sim 9$ ,  $R^4 = 4\pi N$  and  $q$  is a constant which represent the vev of gauge fields condensate [9].  $\Phi$  and  $\chi$  denote the dilaton and the axion respectively. And other field configurations are set to be zero here. The temperature  $T$  is related to the parameter  $r_T$  as  $r_T = \pi R^2 T$ .

In the background given above, we study the dynamical properties of flavor quarks which are introduced as the strings connecting the stacked D3 branes and a newly embedded D7 brane as a probe. The D7 brane is embedded as follows. The six dimensional part of the above metric is rewritten as

$$\frac{1}{f^2(r)} \frac{R^2}{r^2} dr^2 + R^2 d\Omega_5^2 = \frac{R^2}{U^2} \left( d\rho^2 + \rho^2 d\Omega_3^2 + (dX^8)^2 + (dX^9)^2 \right), \quad (4)$$

$$U(r) = \exp \left( \int \frac{dr}{r\sqrt{1 - (r_T/r)^4}} \right) = r\sqrt{\frac{1 + f(r)}{2}}. \quad (5)$$

Here  $U$  is normalized as  $U = r$  for  $r_T = 0$ , and  $U^2 = \rho^2 + (X^8)^2 + (X^9)^2$ . Then we obtain the induced metric for D7 brane,

$$ds_8^2 = e^{\Phi/2} \left\{ \frac{r^2}{R^2} \left( -f^2(r)dt^2 + (dx^i)^2 \right) + \frac{R^2}{U^2} \left( (1 + (\partial_\rho w^8)^2 + (\partial_\rho w^9)^2)d\rho^2 + \rho^2 d\Omega_3^2 \right) \right\}, \quad (6)$$

where  $w^8(\rho)$  and  $w^9(\rho)$  are the scalars which determine the position of D7 brane. They are solved under the ansatz that they depend on only  $\rho$ . Further we can set  $w^9 = 0$  and  $w^8 = w(\rho)$  without loss of generality due to the rotational invariance in  $X^8 - X^9$  plane.

The brane action for the D7-probe is given as

$$S_{D7} = -\tau_7 \int d^8\xi \left( e^{-\Phi} \sqrt{\mathcal{G}} + \frac{1}{8!} \epsilon^{i_1 \dots i_8} A_{i_1 \dots i_8} \right), \quad (7)$$

where  $\mathcal{G} = -\det(\mathcal{G}_{i,j})$ ,  $i, j = 0 \sim 7$ .  $\mathcal{G}_{ij} = \partial_{\xi^i} X^M \partial_{\xi^j} X^N G_{MN}$  and  $\tau_7$  represent the induced metric and the tension of D7 brane respectively. Here we consider the case of

zero  $U(1)$  gauge field on the brane, but we notice that the eight form potential  $A_{i_1 \dots i_8}$ , which is Hodge dual to the axion, couples to the D7 brane minimally. We obtain the eight form potential  $A_{(8)}$  as  $F_{(9)} = dA_{(8)}$  in terms of the Hodge dual field strength  $F_{(9)}$  [17]. By taking the canonical gauge, we arrive at the following D7 brane action,

$$S_{D7} = -\tau_7 \int d^8\xi \sqrt{\epsilon_3} \rho^3 \left( \left( \frac{r}{U} \right)^4 f e^\Phi \sqrt{1 + (w')^2} + C_8 \right), \quad (8)$$

$$C_8 = -\frac{q}{U^4}. \quad (9)$$

Here we notice that  $C_8 \rightarrow -q/r^4 (= 1 - e^\Phi)$  for  $r_T \rightarrow 0$ , and this is consistent with the previous result at  $T = 0$ . We solve the equation of motion for  $w(\rho)$ ,

$$(w - \rho w') \left[ 2(1 - f)^2 - \frac{q}{r^4} e^{-\Phi} \right] + 4w \sqrt{1 + (w')^2} \frac{q}{r^4} e^{-\Phi} - U^2 f \left[ 3 \frac{w'}{\rho} + \frac{w''}{1 + (w')^2} \right] = 0, \quad (10)$$

and find a suitable embedding configuration used in the analysis given here. Here we notice some points with respect to the above action. Firstly we expect that the solutions for  $w$  at  $r_T = 0$  would be smoothly connected to the one of finite  $r_T$  although the horizon appears in the background for finite  $T$ . However we find a phase transition when the end point  $w(0)$  of the solution jumps from  $w(0)$  to  $w(\rho_0)$  where  $\rho_0$  is a point on the horizon. We discuss this point through the embedding solutions.

The solution  $w$  for large  $\rho$  has the asymptotic form

$$w(\rho) \sim m_q + \frac{c}{\rho^2}, \quad (11)$$

where  $m_q$  and  $c$  are interpreted from the gauge/gravity correspondence as the current quark mass and the chiral condensate, respectively. We find that  $w(\rho) = 0$  ( $m_q = 0$  and  $c = 0$ ) is always the solution of (10), and any other solution of nonzero  $m_q$  leads necessarily to nonzero and negative  $c < 0$ . In other words, the chiral symmetry is preserved only for the solution  $w(\rho) = 0$ . We notice however that the sign of nonzero  $c$  is opposite to the case of spontaneous chiral symmetry breaking. This is because of the attractive force between D3 and D7 branes in the present case.

The temperature dependence of the solution is shown in the Fig.1 for  $q = 0$ . We notice that this result is equivalent to the one given in Ref. [5] when  $T$  is replaced by  $m_q$ . This is because of the same form of equations for  $w$  and its independence from the rescaling of all mass dimensional parameters. Actually it is possible to replace  $T$  by  $m_q$  by an appropriate normalization.

We find a jump of the solution near  $T = 1$ , and we expect this as some kind of phase transition. We are already considering in the deconfining phase, so we suppose that there is no hadronic bound state in this phase. However there would be a possible region, as shown below, of the temperature where some hadronic states are still remaining. So, we might expect that a transition from a phase with hadronic states to a phase without any hadronic state would occur at some temperature. Namely, all

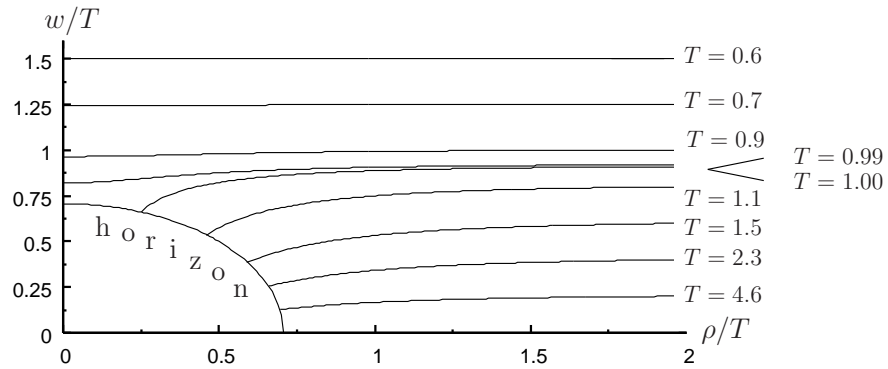


Fig. 1: Embedding solutions for  $q = 0$ . The solutions are drawn for several temperatures, where  $m_q = 0.91$  and  $\pi R^2 = 1$ .

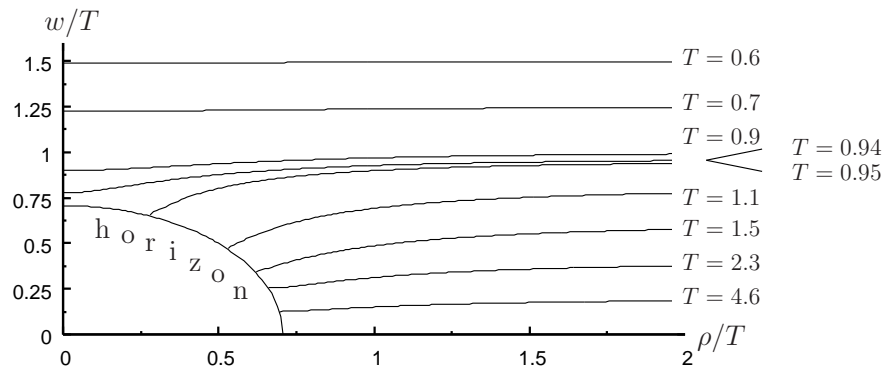


Fig. 2: Embedding solutions for  $q/T^4 = 0.1$  and  $m_q = 0.91$ . The way of the embedding changes at  $T = 0.94 \sim 0.95$  in unit of  $\pi R^2 = 1$ .

the remaining bound states in the high temperature phase disappear above this critical temperature. More on this point, we discuss below and in the following sections.

For  $q \neq 0$ , from the equation (10) we find embedding solutions which are shown in Figure 2. As expected, the gauge field condensate  $q$  affects the critical temperature, and it moves to smaller value than that of the case of  $q = 0$ . This implies that the critical temperature decreases in the presence of the gauge field condensation. This is understood as follows. For nonzero  $q$ , the force becomes small so it would need lower temperature to make the quarks being free than that of the case of  $q = 0$ .

Now we would like to investigate the chiral condensate  $c$  and the energy of D7-brane for the embedding solution. The shape of the solution at high temperature would be determined mainly by the factor  $f(r)$  and the effect from finite  $q$  would be minor. So we study the high temperature solution of  $w$  at  $q = 0$  for simplicity. The chiral condensate depends only on temperature when  $m_q$  and  $R$  are fixed. The absolute value of  $c$  is large at high temperature where the internal coordinates has an endpoint on the horizon. At low temperature, its value becomes small. This behavior is shown in Fig. 3. From

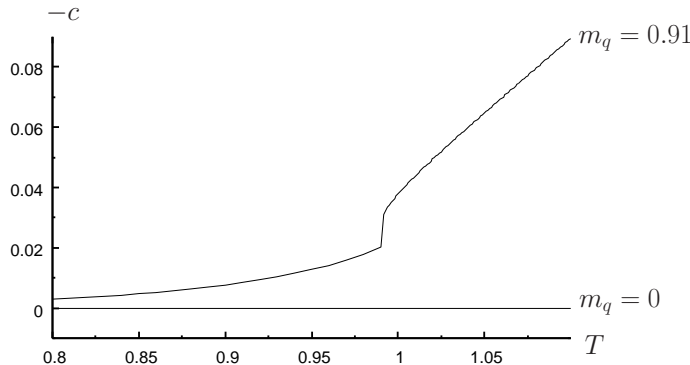


Fig. 3: The temperature dependence of the chiral condensate: for  $m_q = 0.91$  and  $\pi R^2 = 1$ .

in this figure, it is seen that a phase transition occurs at  $T \sim 1$  for  $m_q = 0.91$ . This is consistent with the phase transition which was found by changing the value of  $m_q$  with fixed  $T$  [5].

We turn to temperature dependence of the D7-brane energy. By substituting the background (1)  $\sim$  (3) into the D7-brane action (8), the D7-brane energy for  $q = 0$  is written as

$$E_{D7} = \int_{\rho_{\min}}^{\infty} d\rho \rho^3 \left( 1 - \frac{r_T^8}{16U^8} \right) \sqrt{1 + (w')^2}, \quad (12)$$

which is scaled by  $\tau_7 \sqrt{\epsilon_3}$ . The lower bound  $\rho_{\min}$  is either zero, or, a point on the horizon which the-brane meets. The integral (12) diverges. We regularize it by subtracting the D7-brane energy for  $m_q = 0$  in similar to the analysis given for D4- and D6-branes in

Ref. [3]\*. The regularized energy is

$$\begin{aligned}
E_{\text{reg}} &= E_{\text{D7}}(m_q) - E_{\text{D7}}(0) \\
&= \int_{\rho_{\min}}^{\rho_{\text{match}}} d\rho \rho^3 \left( 1 - \frac{r_T^8}{16U^8} \right) \sqrt{1 + (w')^2} \\
&\quad - \int_{\rho_H}^{\rho_{\text{match}}} d\rho \left( \rho^3 - \frac{r_T^8}{16\rho^5} \right) + \frac{c^2}{\rho_{\text{match}}^2}.
\end{aligned} \tag{13}$$

where  $\rho_H = r_T/\sqrt{2}$  and  $\rho_{\text{match}}$  is the point where we match numerically  $w$  to the asymptotic solution (11). The last term is corrections from the integration for  $\rho > \rho_{\text{match}}$  up to  $\mathcal{O}(\rho_{\text{match}}^{-4})$ . The regularized energy increases monotonically with temperature. For fixed  $m_q$ , the slope  $dE_{\text{reg}}/dT$  has a discontinuous jump at  $T = T_{\text{fund}}$ . Fig. 4 shows the temperature dependence of the regularized energy. It is clear that the lowest D7-brane

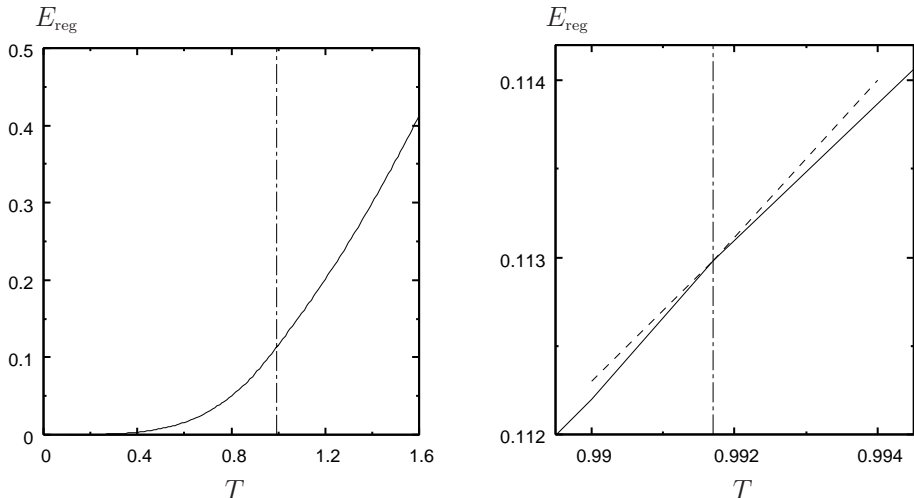


Fig. 4: The temperature dependence of the regularized energy: for  $m_q = 0.91$  and  $\pi R^2 = 1$ . The vertical line denotes  $T = T_{\text{fund}}$ . The right figure shows the neighborhood of the transition point. The dashed lines stand for the slopes at the transition point.

energy is obtained for the case where the current quark mass is zero. For  $m_q \neq 0$ , the energy depends on whether the end point of  $w$  is on the horizon or not. At high temperature side,  $T > T_{\text{fund}}$ , the energy of the solution which meet the horizon becomes lower than the one of the other type solution.

As we will show, the solution attached to the horizon leads to vanishing of dynamical quark mass and then of the quark-antiquark potential. Then the change of phase at  $T = T_{\text{fund}}$  will be regarded as the phase transition from the phase with surviving hadronic states to the free-quark phase. This point will be discussed more in the followings.

\*Note that the chiral condensate and the regularized energy in Ref. [3] are rescaled by the temperature.

### 3 Quark-antiquark potential

We study a gravity description of quark-antiquark potentials in detail. Before performing concrete calculations, we review how quark-antiquark potentials are described in the context of the gauge/gravity correspondence. The point relevant to the present purpose is in the following.

We consider the Wilson-Polyakov loop in  $SU(N)$  gauge theory:

$$W = \frac{1}{N} \text{Tr} P e^{i \int A_0 dt}. \quad (14)$$

The quark-antiquark potential  $V_{q\bar{q}}$  is derived from the expectation value of a parallel Wilson-Polyakov loop:

$$\langle W \rangle \sim e^{-V_{q\bar{q}} \int dt}. \quad (15)$$

On the other hand, the dual gravity suggests that the expectation value is represented as

$$\langle W \rangle \sim e^{-S}, \quad (16)$$

in terms of the Nambu-Goto action

$$S = -\frac{1}{2\pi\alpha'} \int d\tau d\sigma \sqrt{-\det h_{ab}}, \quad (17)$$

with the induced metric

$$h_{ab} = G_{\mu\nu} \partial_a X^\mu \partial_b X^\nu, \quad (18)$$

where the string coordinate is  $X^\mu(\tau, \sigma)$  and the string world-sheet is parameterized by  $\sigma, \tau$ . From the equations (15) and (16), the quark-antiquark potential can be calculated by setting various configurations of string coordinates and background geometries. In the following analysis, we investigate quark-antiquark potentials by considering static string configurations.

#### 3.1 Gauge-field condensate model

We examine quark-antiquark potentials in the background presented here. To study possible static string configurations of a pair of quark and anti-quark, we choose  $X^0 = t = \tau$  and decompose the other nine string coordinates into components parallel and perpendicular to the D3-branes:

$$\mathbf{X} = (\mathbf{X}_{||}, r, r\Omega_5). \quad (19)$$

The Nambu-Goto Lagrangian in the background (1) becomes

$$L_{\text{NG}} = -\frac{1}{2\pi\alpha'} \int d\sigma e^{\Phi/2} \sqrt{r'^2 + r^2 f(r)^2 \Omega_5'^2 + \left(\frac{r}{R}\right)^4 f(r)^2 \mathbf{X}_{||}'^2}, \quad (20)$$

where the prime denotes a derivative with respect to  $\sigma$ . The test string has two possible configurations: (i) a pair of parallel strings, which connect horizon and the D7 brane, and (ii) a U-shaped string whose two end-points are on the D7 brane.

We firstly consider the configuration (i) of parallel two strings, which have no correlation each other. The total energy is then two times of one dynamical quark mass,  $\tilde{m}_q$ . As mentioned above, it is given by a string configuration which stretches between the horizon  $r_T$  and the maximum  $r_{\max}$ , so we can take as

$$r = \sigma, \quad \mathbf{X}_{\parallel} = \text{constant}, \quad \Omega_5 = \text{constant}. \quad (21)$$

Then  $\tilde{m}_q$  is obtained by substituting (21) into (20) as follows,

$$E = \frac{1}{\pi\alpha'} \int_{r_T}^{r_{\max}} dr e^{\Phi/2} = 2\tilde{m}_q. \quad (22)$$

The temperature dependence of the dynamical mass  $\tilde{m}_q$  is shown in Fig. 5.

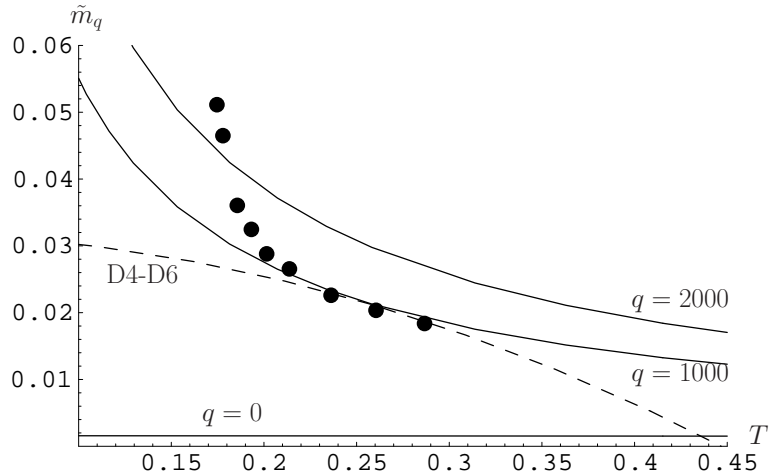


Fig. 5:  $\tilde{m}_q$  are shown for  $R = 1/\sqrt{\pi}(\text{GeV}^{-1})$ ,  $r_{\max} = 10(\text{GeV}^{-1})$  and  $\alpha' = 10^3(\text{GeV}^{-2})$ . The three solid curves are corresponding to the case of  $q = 0$ ,  $10^3$  and  $2 \times 10^3(\text{GeV}^{-4})$ , respectively. The dashed curve represents the result for the D4-D6 model (33) with  $R = 10(3/4\pi)^{2/3}$ ,  $r_{\max} = 200$  and  $\alpha' = 10^3$ . The points represent the lattice data [18].

Generally,  $r_{\max}$  depends on temperature. However, when temperature is low, its change is very small. Therefore we set approximately constant  $r_{\max}$ . The points are quoted from the lattice data of Fig. 5 in reference [18]: we regard the asymptotic values of the heavy quark free energy as the sum of two dynamical quark masses. <sup>†</sup> The behavior of our result is resemble to the lattice behavior because of the concave shape. Especially, putting  $R = 1/\sqrt{\pi}(\text{GeV}^{-1})$ ,  $q = 10^3(\text{GeV}^{-4})$ ,  $r_{\max} = 10(\text{GeV}^{-1})$  and  $\alpha' = 10^3(\text{GeV}^{-2})$ , the dynamical mass (22) corresponds to the lattice results at least for the region  $0.2 \lesssim T \lesssim 0.3(\text{GeV})$ . Although  $\alpha'$  has to become small, we can fit the result of the model to the lattice data only at a large value i.e.  $\alpha' = 10^3(\text{GeV}^{-2})$ . This situation is an open problem here.

<sup>†</sup>We convert the data by use of  $T_c \cong 0.173 \text{ GeV}$  and  $T_c/\sqrt{\sigma} \cong 0.425$ , where  $\sigma$  is a string tension.

For  $q = 0$ , temperature dependence of  $\tilde{m}_q$  is not seen, but it largely affected by  $T$  for  $q \neq 0$ . And, at any point of  $T$ ,  $\tilde{m}_q$  increases with  $q$ . We should notice that  $\tilde{m}_q$  disappears when the temperature exceeds  $T_{\text{fund}}$ , the D3-brane is included in the D7-brane.

We now turn to the U-shaped configuration,

$$\mathbf{X}_{||} = (\sigma, 0, 0), \quad \Omega_5 = \text{constant}. \quad (23)$$

The equation of motion derived from the Lagrangian (20) with the configuration (23) are solved by

$$e^{\Phi/2} \frac{1}{\sqrt{(r/R)^4 f(r)^2 + (dr/d\sigma)^2}} \left(\frac{r}{R}\right)^4 f(r)^2 = \text{constant}. \quad (24)$$

The midpoint  $r_0$  of the string is determined by  $dr/d\sigma|_{r=r_0} = 0$ . Then the distance and the total energy of the quark and anti-quark are given by

$$L = 2R^2 \int_{r_0}^{r_{\max}} dr \frac{1}{r^2 f(r) \sqrt{e^{\Phi(r)} r^4 f(r)^2 / (e^{\Phi(r_0)} r_0^4 f(r_0)^2) - 1}}, \quad (25)$$

$$E = \frac{2}{\pi \alpha'} \int_{r_0}^{r_{\max}} \frac{e^{\Phi(r)/2}}{\sqrt{1 - e^{\Phi(r_0)} r_0^4 f(r_0)^2 / (e^{\Phi(r)} r^4 f(r)^2)}}. \quad (26)$$

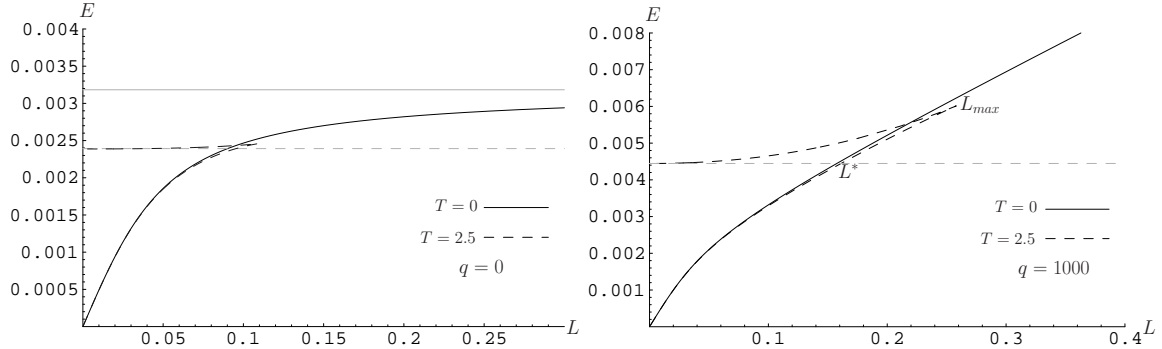


Fig. 6: Plots of  $E$  vs  $L$  at  $q = 0$  and  $q = 10^3(\text{GeV}^{-4})$  for  $R = 1/\sqrt{\pi}(\text{GeV}^{-1})$ ,  $r_{\max} = 10(\text{GeV}^{-1})$  and  $\alpha' = 10^3(\text{GeV}^{-2})$ . The solid and dashed curves represent the case of  $T = 0$  and  $T = 2.5(\text{GeV})$ , respectively. The vertical solid and dashed lines represent the energy of two parallel straight strings.

Figure 6 shows the dependence of the energy  $E$  on the distance  $L$  at some selected temperatures  $T$  and  $q$ . The results at  $q = 0$  (left Fig. 6) are consistent with the one given in reference [12], where infinitely heavy quarks are considered. However, we consider the quark with a light mass, not the heavy quark, we then need not to consider the energy difference between the U-shape string and a pair of strings as in [12].

For the case of finite  $q$  (the right Fig. 6), we can see the linear rising potential for  $T = 0$ , and it shows the confinement of quark and antiquark. On the other hand, for finite temperature  $T = 2.5$ , the qualitative behavior coincides with the one of  $q = 0$ . Namely,  $E$  increases with  $L$  along the curve of  $T = 0$  but the potential disappears at  $L = L_{max}$ , which depends on the temperature. More important fact is that  $E$  exceeds the energy of the two straight strings configuration at  $L = L^* < L_{max}$ . When  $L \geq L^*$ , the straight strings configuration has a lower energy than the U-shaped string configuration. As the two straight strings have no interaction energy, this shows that the quark-antiquark potential vanishes for  $L \geq L^*$ . So there will be no physical meaning the potential obtained in the region of  $L^* < L < L_{max}$ . This characteristic behavior is qualitatively in agreement with the suggestions given by lattice simulations [18].

### 3.2 D4-D6 model

Next, we calculate the quark-antiquark potential by using the D4-D6 model [4]. The type IIA supergravity background dual to  $N_c$  D4-branes compactified in a circle with anti-periodic boundary conditions for the fermions at high temperatures takes the form

$$ds^2 = \left(\frac{r}{R}\right)^{3/2} \left(-\tilde{f}(r)dt^2 + \sum_{i=1}^3 dx^i dx^i + d\tau^2\right) + \left(\frac{R}{r}\right)^{3/2} \frac{dr^2}{\tilde{f}(r)} + R^{3/2} r^{1/2} d\Omega_4^2, \quad (27)$$

$$e^\Phi = \left(\frac{r}{R}\right)^{3/4}, \quad \tilde{f}(r) = 1 - \frac{r_T^3}{r^3}, \quad (28)$$

at high temperature. The coordinates  $(t, x^1, x^2, x^3)$  parametrize the four directions along the D4-branes and time-coordinate  $t$  is compactified with the period  $1/T$ . The coordinate  $\tau$  parametrizes the circular 4th-direction on which the branes are compactified.  $d\Omega_4^2$  is the  $SO(5)$ -invariant line element.  $r$  has dimensions of length and is regarded as a radial coordinate in the 56789-directions transverse to the D4-branes. Since we wish to avoid conical singularities at  $r = r_T$ , the boundary condition fixes the metric parameter as

$$r_T = \left(\frac{4\pi T}{3}\right)^2 R^3. \quad (29)$$

We take  $X^0 = t$  and decompose the nine spatial embedding coordinates as follows:

$$\mathbf{X} = (\mathbf{X}_{||}, T, r, r\Omega_4) \quad (30)$$

In this case, The Nambu-Goto Lagrangian in a static configuration becomes

$$L_{NG} = -\frac{1}{2\pi\alpha'} \int d\sigma \sqrt{r'^2 + \tilde{f}(r)r^2\Omega_4'^2 + \left(\frac{r}{R}\right)^3 \tilde{f}(r)(\mathbf{X}'^2 + T'^2)}. \quad (31)$$

As in previous section, we set the embedding coordinates for a pair of straight strings which are stretched between D4-branes and D6-brane as follows:

$$r = \sigma, \quad \mathbf{X}_{||} = \text{constant}, \quad T = \text{constant}, \quad \Omega_4 = \text{constant}, \quad (32)$$

so that we obtain the total energy of the quark-antiquark pair

$$E = \frac{1}{\pi\alpha'}(r_{\max} - r_T) = 2\tilde{m}_q . \quad (33)$$

Because the position of the horizon  $r_T$  is proportional to the square of temperature, the temperature dependence of the dynamical quark mass  $\tilde{m}_q$  has a convex form (see Fig.5). This form is considerably different from the tendency of the lattice result and also from the result our gauge-field condensate model. Also, the dynamical mass becomes zero before the horizon approaches to the D6-brane and this tendency is different from the gauge-field condensate model.

For the U-shape string configuration, we set the embedding coordinates as follows:

$$\mathbf{X}_{||} = (\sigma, 0, 0) , \quad T = \text{constant} , \quad \Omega_4 = \text{constant} . \quad (34)$$

From the equation of motion for the coordinates  $\mathbf{X}_{||}$ , we obtain the distance between quark and antiquark

$$L = \frac{2R^{3/2}\sqrt{r_{\min}^3 - r_T^3}}{r_T^{1/2}} \int_{r_{\min}}^{r_{\max}} \frac{dr}{\sqrt{(r^3 - r_T^3)(r^3 - r_{\min}^3)}} , \quad (35)$$

and, from the Hamiltonian, we obtain the total energy of the U-shape string of inter-quark separation  $L$

$$E = \frac{1}{\pi\alpha'} \int_{r_{\min}}^{r_{\max}} dr \sqrt{\frac{r^3 - r_T^3}{r^3 - r_{\min}^3}} . \quad (36)$$

Fig.7 shows the dependence of the energy  $E$  on the distance  $L$  at temperatures  $T = 0$  and  $T \neq 0$ . In this case, both behaviors are equivalent to our gauge condensate model.

## 4 Possible hadron spectrum at high temperature

### 4.1 Screening mass

One of the basic characteristics of a plasma is the screening of color electric fields. In the paper [12], the asymptotic behavior of the heavy quark potential at large distance  $L$  is given as follows;

$$V_{\text{BN}}(L, T) \approx -C_M \frac{e^{-m_{\text{sc}}L}}{L} + \dots , \quad (37)$$

where  $m_{\text{sc}} \propto T$  is a screening mass. In this section, we investigate the temperature dependence of the screening mass in both the gauge-field condensate model and the D4-D6 model by comparing the quark-antiquark potential to Eq. (37). The quark-antiquark potential in the gauge-field condensate model is given by

$$V_{q\bar{q}}(L, T) = E(L, T) - 2\tilde{m}_q . \quad (38)$$

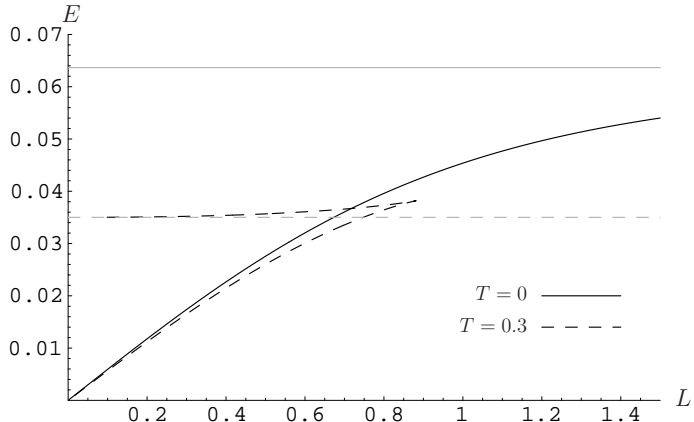


Fig. 7: The energy  $E$  vs  $L$ , for  $R = 10(3/4\pi)^{2/3}$ ,  $r_{\max} = 200$  and  $\alpha' = 10^3/GeV^2$ . The solid and dashed curves represent the energy at  $T = 0$  and  $T = 0.3$ , respectively. And the solid and dashed lines represented the energy of two straight strings at  $T = 0$  and  $T = 0.3$ , respectively.

Comparing the two potentials (38) and (37) at distance  $L^*$ , we obtain the temperature dependence of the screening mass as figure 8<sup>‡</sup>: In the gauge-field condensate model, the screening mass is almost proportional to the temperature. This result coincides with the result given in Ref. [21]. While in the D4-D6 model, the screening mass almost becomes zero in  $T \sim 0.19$ . It is considered that the reason of this result is because quark and antiquark do not completely confine even at  $T = 0$ . As the temperature increases, the screening mass is almost proportional to the temperature until  $T \sim 0.27$  and shapely increases when the temperature exceeds 0.27. This result is different from the one given in Ref. [21].

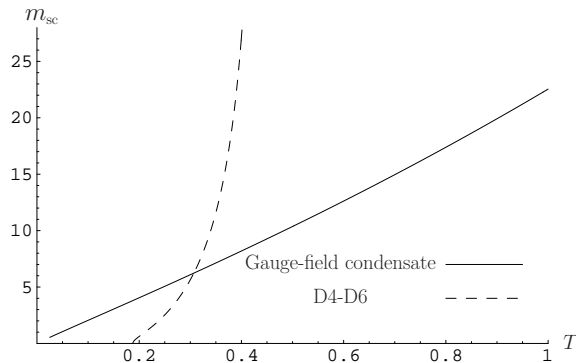


Fig. 8: The temperature dependence of the screening mass: the solid curve represents the result of the Gauge-field condensate model, while the dashed curve represents the result of the D4-D6 model.

<sup>‡</sup>We do not treat the high temperature region because  $L^*$  becomes too small to use the results (37).

## 4.2 Meson

In this section, we consider about the meson spectra. As mentioned in the end of section 3.1, when  $L \leq L^*$  the energy of the U-shape string becomes lower than the energy of the pair strings, while when  $L \geq L^*$  the result reverses. This result shows that when the distance between quark and antiquark is close, these quarks are confined, while the distance becomes wide and moreover exceeds  $L^*$ , deconfinement occurs and the energy becomes two quark masses. Therefore we can obtain effective potential like Fig.9. According to Fig.9, as temperature increase, possibility of existence of meson spectra, which shall exist certainly at  $T = 0$ , become lower and lower, because the height of the potential becomes shallower, namely, the region in which mesons can exist becomes more narrow. Especially, when the temperature exceeds  $T_{\text{fund}}$ , the potential identically becomes zero. This leads to the deconfinement.

We investigate this fact by a simple manner: we solve the 3-dimensional Schrödinger equation with this effective potential and investigate the bound states [13, 14]. As a result, we could show that the bound states i.e. the meson spectra exist for  $T \sim 0.043$  in the gauge-field condensate model.

Also, for comparison, utilizing the lattice data quoted from Fig. 3 in reference [18], we can investigate the bound states: the heavy quark free energy converges finite value for long distance between quark. Therefore, we may regard the value as the mass of a pair of effective quark and antiquark, which are not confining. Deforming the free energy so that we can regard the asymptotic value as zero and using it as the potential of the Schrödinger equation, we show a result that the bound states exist for less than the critical temperature  $T_{\text{fund}}$ .

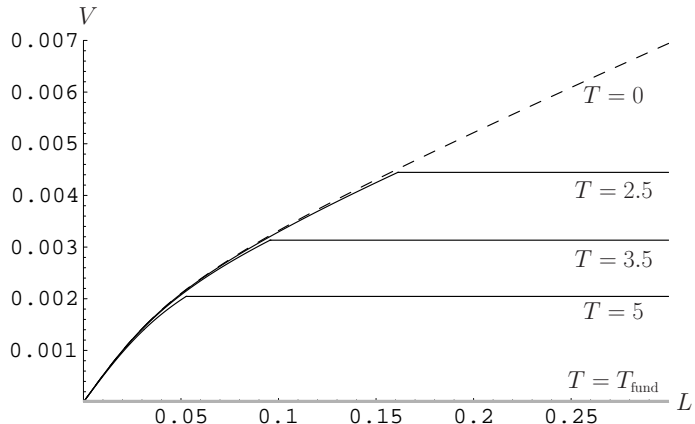


Fig. 9: The effective quark-antiquark potential  $V$  for  $R = 1/\sqrt{\pi}(\text{GeV}^{-1})$ ,  $q = 10^3(\text{GeV}^{-4})$ ,  $r_{\text{max}} = 10(\text{GeV}^{-1})$  and  $\alpha' = 10^3(\text{GeV}^{-2})$ . The dashed curve represents the result for  $T = 0$  and the solid curves represent the results for  $T = 2.5, 3.5$  and  $5$ , respectively.

### 4.3 Baryon

It has been shown that baryons correspond to D5-branes wrapped around the compact manifold  $M_5$  [19, 20]. As a typical case, here we take  $S^5$  and investigate the qualitative property. The brane action of such a D5 probe is

$$S_{D5} = -\tau_5 \int d^6\xi e^{-\Phi} \sqrt{\mathcal{G}} , \quad (39)$$

where  $(\xi_i) = (X^0, X^5 \sim X^9)$ ,  $\tau_5$  represents the tension of D5 brane, and  $\mathcal{G} = -\det(\mathcal{G}_{ij})$  for the induced metric  $\mathcal{G}_{ij} = \partial_{\xi^i} X^M \partial_{\xi^j} X^N G_{MN}$ . The mass of the wrapped D5-brane is then

$$M_{D5}(r) = \tau_5 e^{-\Phi} \sqrt{\mathcal{G}} = \tau_5 \pi^3 R^4 r f(r) e^{-\Phi/2} . \quad (40)$$

The mass  $M_{D5}$  thus defined depends on the position  $r$  of the D5-brane. As for  $T = 0$ ,  $M_{D5}$  has a simple form

$$M_{D5}(r) = \tau_5 \pi^3 R^4 r \sqrt{1 + \frac{q}{r^4}} . \quad (41)$$

The  $M_{D5}(r)$  diverges at both  $r = 0$  and  $r = \infty$ , and it has a global minimum  $M_{D5}(r_{\min}) = \tau_5 \pi^3 R^4 (4q)^{1/4}$  at  $r = r_{\min} = q^{1/4}$ ; see the dashed curve in Fig. 10. The minimum value can be regarded as the baryon mass from the action principle. In the AdS limit, namely  $q \rightarrow 0$ , the baryon mass vanishes. Thus, the baryon mass is induced by finite  $q$ , i.e. by finite gauge-field condensate, in this model.

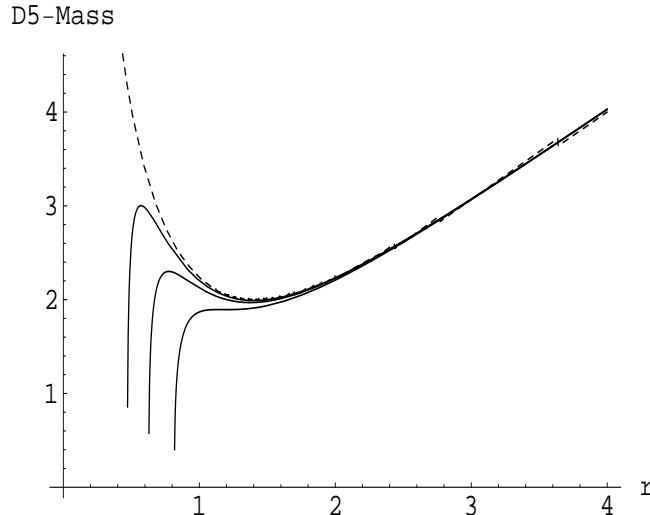


Fig. 10: The D5-brane mass  $M_{D5}(r)$  as a function of  $r$ . Here we set  $q = 4$ .  $M_{D5}(r)$  and  $T$  are shown in units of  $\tau_5 \pi^3 R^4$  and  $R^{-2}$ , respectively. The dashed curve shows the case of  $T = 0$ , and three solid curves represent cases of  $T = 0.15, 0.2, 0.26$ , respectively, from left to right.

As for  $T > 0$ ,  $M_{D5}(r)$  has a form

$$M_{D5}(r) = \tau_5 \pi^3 R^4 r \sqrt{\left(1 + \frac{q}{r_T^4} \log\left(\frac{1}{1 - (r_T/r)^4}\right)\right) \left(1 - \frac{r_T^4}{r^4}\right)} . \quad (42)$$

The  $M_{D5}(r)$  is real only for  $r \geq r_T$ . In the region,  $M_{D5}(r)$  is zero at  $r = r_T$  and positive for  $r > r_T$ . Thus, even if a minimum exists at  $r > r_T$ , it is only a local minimum; see the solid curves in Fig. 10. One could regard the local minimum as baryon, but the baryon is metastable when  $T$  is finite.

Figure 10 shows the  $r$  dependence of  $M_{D5}(r)$  for four values of  $T$ . When  $T = 0$ , there exists a minimum at  $r = q^{1/4} = 1$ , as mentioned above. The minimum becomes a local minimum for  $T < 0.26$ , and eventually it disappears for  $T > 0.26$ . Thus, baryon can survive as a metastable state for small  $T$ . Furthermore, we can see from Fig. 10 that the mass of the metastable baryon is almost independent of  $T$ .

## 5 Summary

A gauge theory with light flavor quarks is studied in a dual supergravity of the AdS background deformed by dilaton, which induces the gauge-field condensate in the dual gauge theory. The high-temperature-phase background is constructed by making the AdS-Schwarzshild compactification. This background, at zero temperature limit, corresponds to a dual of the  $\mathcal{N} = 1$  supersymmetric gauge theory with the quark confinement [9].

Introducing the flavor quark by embedding the D7 probe brane in this high-temperature background, we found no spontaneous chiral symmetry breaking in this case. Furthermore, through the analysis of the Wilson-Polyakov loop, we found that the dynamical quark mass is not divergent and the quark-antiquark potential has a finite range. Thus, these properties are consistent with the one of high temperature QCD phase.

It might be a new point that, in this deconfinement phase, there exists still a phase transition at a temperature,  $T_{\text{fund}}$ . It is observed through the temperature dependence of the D7 brane energy and the vev of quark bilinear. In the gravity side, this transition is seen through the form of the embedded D7 brane when its end-point meets with the horizon. This transition takes place for both cases with and without gauge-field condensate, and the similar transition is also seen in other models [4, 5]. Hence, this transition would be universal.

In the higher temperature phase ( $T > T_{\text{fund}}$ ), both the dynamical quark mass and the potential between quark and antiquark vanish. This implies that the phase is in a quark-gluon plasma. Meanwhile, in the lower temperature phase ( $T < T_{\text{fund}}$ ), the dynamical quark mass is finite and a short ranged interaction between quark and antiquark still remains. In consequence, quark bound states are possible. The bound states would be atom-like in the sense that each constituent can be separated, and these bound states disappear above the critical temperature  $T_{\text{fund}}$ . Similar property can be seen for baryon, which is studied here by D5 brane embedded in the high-temperature background.

As for the dynamical quark mass, its temperature dependence is compared with the numerical results of full lattice QCD, and we found that our result is qualitatively consistent with the lattice data. The temperature dependence of the screening mass is also investigated. We find that the screening mass increases linearly with temperature

in our present model [21]. This is also consistent with the analysis given in real QCD. The present analysis is valid in the large  $N_c$  limit and D7 brane is treated as a probe. In this sense, our analysis is akin to the quenched approximation, namely the quark-antiquark creation is not included in our analysis. However this would not affect the qualitative property of our results, since the qualitative property of the analyses is not changed so much between full lattice QCD and quenched lattice QCD [22].

Thus, we could say that there are good correspondences between the deconfinement phase of the present background and that of real QCD. Finally we should comment on the unwanted modes which are not seen in the real QCD. Here we start from IIB superstring theory, and the action for the D7 brane includes fermionic fields as the super-partner. These fermionic modes do not correspond to any baryonic state in real QCD. So we expect that the masses of these state would be large and decouple to our low energy theory. But this point is open at present stage.

## Acknowledgments

This work has been supported in part by the Grants-in-Aid for Scientific Research (13135223, 14540271) of the Ministry of Education, Science, Sports, and Culture of Japan. This work is also in part by the Grant-in-Aid for Scientific Research on Priority Areas "Progress in elementary particle physics of the 21st century through discoveries of Higgs boson and supersymmetry" (No.441).

## References

- [1] J. M. Maldacena, *Adv. Theor. Math. Phys.* **2**, 231 (1998) [hep-th/9711200].  
 S. S. Gubser, I. R. Klebanov and A. M. Polyakov, *Phys. Lett. B* **428**, 105 (1998) [hep-th/9802109].  
 E. Witten, *Adv. Theor. Math. Phys.* **2**, 253 (1998) [hep-th/9802150]. A.M. Polyakov, *Int. J. Mod. Phys. A* **14** (1999) 645, (hep-th/9809057).
- [2] A. Karch and E. Katz, *JHEP* **0206**, 043(2003) [hep-th/0205236].
- [3] M. Kruczenski, D. Mateos, R.C. Myers and D.J. Winters, *JHEP* **0307**, 049(2003) [hep-th/0304032].
- [4] M. Kruczenski, D. Mateos, R.C. Myers and D.J. Winters, [hep-th/0311270].
- [5] J. Babington, J. Erdmenger, N. Evans, Z. Guralnik and I. Kirsch, hep-th/0306018.
- [6] N. Evans, and J.P. Shock, *Phys. Rev.* **D70**, 046002 (2004).
- [7] T. Sakai and J. Sonnenschein, *JHEP* **0309**,047 (2003).
- [8] C. Nunez, A. Paredes and A.V. Ramallo, *JHEP* **0312**, 024(2003) [hep-th/0311201].

- [9] K. Ghoroku and M. Yahiro, Phys. Lett. **B604**, 235 (2004).
- [10] T. Sakai and S. Sugimoto, hep-th/0412141.
- [11] D. Bak and H. Yee, Phys. Rev. D71 (2005) 046003 [hep-th/0412170].
- [12] S.J. Rey, S. Theisen and J.T. Yee, Nucl. Phys. B527(1998)171.
- [13] O.J.P. Eboli, R. Jackiw and S.-Y. Pi, Phys. Rev. **D37**, 3557 (1988).
- [14] G.P. Malik, R.K. Jha and V.S. Varma, Astroph. J. **503**, 446 (1998); Eur. Phys. J. **A2** 105, (1998).
- [15] A. Kehagias and K. Sfetsos, Phys. Lett. B **456**, 22(1999) [hep-th/9903109].
- [16] H. Liu and A.A. Tseytlin [hep-th/9903091].
- [17] G. W. Gibbons, M. B. Green and M. J. Perry, Phys. Lett. B370 (1996) 37-44, [hep-th/9511080].
- [18] O. Kaczmarek, S. Ejiri, F. Karsch, E. Laermann, F. Zantow, Prog. Theor. Phys. Suppl. **153**, 287 (2004); P. Petreczky, K. Petrov, Phys. Rev. **D70**, 054503 (2004).
- [19] D. J. Gross and H. Ooguri, Phys. Rev. **D58**, 106002(1998) [hep-th/9805129].
- [20] E. Witten, JHEP **7**, 006(1998) [hep-th/9805112].
- [21] E. Braaten and A. Nieto, Phys. Rev. Lett. 74 (1995) 3530.
- [22] O. Kaczmarek, S. Karsch, E. Laermann, M. Lütgemeier, Phys. Rev. **D62** 034021 (2000).